PHYSICAL REVIEW B VOLUME 16, NUMBER 4 15 AUGUST 1977

Intrinsic and extrinsic plasmon coupling in x-ray photoemission from core states of adsorbed atoms

A. M. Bradshaw
Fritz-Haber-Institut der Max-Planck-Gesellschaft, Faradayweg 4-6, West Berlin 33, Germany

W. Domcke* and L. S. Cederbaum*
Physik-Department (T30) der Technischen Universität München, James-Franck-Strasse, 8046 Garching, West Germany
(Received 8 September 1976)

The coupling of a surface plasmon to an adsorbate core level in x-ray photoelectron spectroscopy has been observed for the 1*s* level of oxygen adsorbed on an aluminum (111) surface. The coupling parameter was found to be strongly coverage dependent. To distinguish between intrinsic and extrinsic effects the dependence of the coupling parameter on the photoelectron escape angle was also measured. In this way both extrinsic and intrinsic terms could be identified, as well as the interference term. Within the framework of the model used for the interpretation of results, the intrinsic effect was found to be low in magnitude with a coupling parameter of ~0.04, which implies a surface-plasmon screening energy of about 0.4 eV. This unexpectedly weak core-hole-plasmon coupling is explained by considering the repulsion of the screening charge by the valence electrons of the adsorbed atom.

I. INTRODUCTION

X-ray photoelectron spectra (XPS) of solids invariably reveal satellites on the low-kinetic-energy side of characteristic core level lines. These satellites may be extrinsic in origin,[1] that is, they may be due to discrete energy losses associated with the movement of the photoelectrons from the site of excitation through the solid to the surface. The fast electron can, for example, excite surface and bulk plasmons or, alternatively, induce single-particle transitions. An understanding of the extrinsic effect is necessarily relevant to the problem of hot-electron scattering lengths and mean escape depths, which in turn are important for quantifying the XPS technique.[2] On the other hand, satellites or structure in the spectrum may occur due to excitations (collective or single-particle) which take place during the ionization event itself. These are termed "intrinsic."[1] The presence of intrinsic volume-plasmon satellites, for example, in the core level spectra of carbon and the *s* metals has been discussed at length during the last three years.[3-10] The importance of intrinsic coupling lies in its relation to relaxation effects. When part of the spectral density is distributed over intrinsic satellite lines, the center of gravity of the spectrum will yield the "frozen" core electron energy (or "Koopmans' energy") as opposed to the relaxed energy of the core electron given by the position of the "adiabatic" peak.[1,11,12]

In a recent analysis of the loss structure on the 2*s* and 2*p* lines in the x-ray photoelectron spectra of sodium, magnesium, and aluminum Pardee *et al.*[9] were led to the conclusion that no intrinsic plasmons could be identified. Moreover the presence of any other intrinsic structure appeared unlikely due to the choice of background necessary for the analysis of the data. However, the so-called extra-atomic relaxation contribution to the core level binding energies in aluminum metal has been estimated to be as high as 5 eV.[13] Fuggle *et al.*,[10] who noted this paradox, have sought to distinguish between intrinsic and extrinsic plasmons by studying the spectra of successively evaporated aluminum films on a manganese substrate. The plasmon satellites on the 2*s* level of aluminum were found to have some intrinsic character, but uncertainty as to the structure of the aluminum overlayer prevented a quantitative analysis.

In the present paper we consider a somewhat simpler system, namely, the coupling of a *surface* plasmon to an *adsorbate* core level. This problem has recently been discussed theoretically by Harris[14] and by Gumhalter and Newns.[15] The first clear observation[16] of such an effect is described here for the system oxygen–aluminum (111). Since the background problems are less severe than in the bulk case and since the angular dependence of the coupling strength can be analyzed in terms of a well-defined theoretical model, the intrinsic contribution can be identified and quantitatively estimated. In view of the recent interest in screening effects in photoemission from adsorbate layers,[17] experiments of this nature are presently of some relevance.

II. EXPERIMENTAL

X-ray photoemission data was taken on an AEI 200A photoelectron spectrometer with a base

pressure of $(2-3)\times10^{-10}$ Torr. The sample was an aluminum-single-crystal slab ($12\times4\times1$ mm^3) with its rotational axis accurately positioned parallel to the entrance slit in the normal plane of the hemispherical electron energy analyzer. Under the chosen operating conditions the acceptance angular apertures in the dispersion and normal planes at a kinetic energy of 730 eV were below 1° and 5°, respectively, thus making the instrument suitable for XPS angular distribution studies.[18] The aluminum single crystal (Metals Research 99.9999% pure) had been oriented to within $\frac{1}{2}$° of the (111) plane, cut by spark erosion and reoriented on the polishing jig subsequent to mechanical polishing with successively finer diamond pastes. The final stage was an electropolish in a perchloric-acid–acetic-anhydride solution, which left a bright mirror finish as well as several isolated etch pits. *In situ* cleaning consisted of argon-bombardment–annealing cycles lasting for several days (anneal temperature 450°C). Residual oxygen was monitored with XPS: a surface oxygen impurity concentration of 0.03 ML (Monolayer) could not be improved upon.

Oxygen exposures were performed at room temperature and at 2×10^{-7} Torr or lower. Higher pressures resulted in pressure-dependent chemisorption and oxidation rates. The chemisorption kinetics were investigated using the integrated intensity of the O 1*s* peak and will be reported in detail elsewhere.[19] Monolayer coverage was defined as the point at which the O 1*s* peak begins to broaden and shift to higher binding energies. The O 1*s* binding energy during the initial stages of interaction up to an exposure of 50 langmuir (1 L $=10^{-6}$ Torr sec) was found to be 531.3 ± 0.2 eV as opposed to 532.4 ± 0.2 eV after formation of a thick oxide layer. The respective peak half widths were 1.4 and 2.2 eV. Thus evidence exists for two stages in the interaction, a first stage presumably consisting of oxygen chemisorption and a second stage involving nucleation of oxide particles leading eventually to the formation of an oxide film.

The O 1*s* peak on Al(111) after an exposure of 5 L and at a photoelectron escape angle of 15° is shown in Fig. 1. The coverage is estimated on the basis of the above criteria to be 0.17 monolayers. The spectrum was recorded by multiple scanning using a Nicolet signal averager. Total scan time was 3 h. Longer scan times were found to alter the form of the O 1*s* peak, probably due to the presence of coadsorbed water vapor.[20] The satellite at 10.9 eV we attribute to the aluminum surface plasmon, which can also be observed clearly on the aluminum 2*s* and 2*p* lines at the same energy (see for example Fig. 2). Although a further broad loss can be detected at 24 eV,[21] there is no evidence

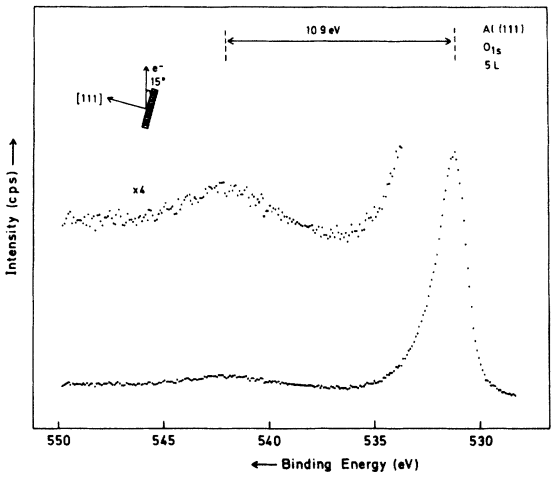

FIG. 1. O 1*s* peak from the XPS spectrum of an aluminum (111) after chemisorption with oxygen to a coverage of 0.17 ML. Mean electron escape angle: 15°. Source radiation: Mg $K\alpha$.

for a coupling to the volume plasmon as observed on the aluminum lines. The fact that coupling occurs *only* to the surface plasmon suggests, in terms of both intrinsic and extrinsic coupling models, that oxygen remains outside the surface during the initial interaction in clear contradiction to current opinion as to the nature of the adsorption process on aluminum. Thus in recent years several authors have interpreted data from polycrystalline surfaces in terms of either reconstruction or direct incorporation into the bulk.[20,22-25] Unfortunately little direct evidence is available to support these assumptions, largely because low-energy-electron diffraction investigations have given no definitive insight into the surface crystallography of the aluminum-oxygen system.[26] The intensity of the surface plasmon satellite relative to the main line decreases with increasing coverage during the initial chemisorption stage. As oxidation proceeds (after 50 L at 2×10^{-7} Torr) the surface plasmon energy shifts to lower values, ending up at 7.8 eV which corresponds to the interface plasmon for the aluminum-aluminum-oxide interface.[27] A similar effect has been observed in electron-energy-loss investigations of aluminum oxidation.[28-30] A recent report in the literature suggests that such effects can also be observed on transition-metal surfaces.[31]

The coverage dependence of the surface plasmon coupling parameter is somewhat difficult to measure accurately. As a guide to the magnitude of this effect we note that the coupling parameter at 1.0 ML is approximately one-third of its value at 0.2 ML for a given photoelectron escape angle. The same effect can, however, be observed more

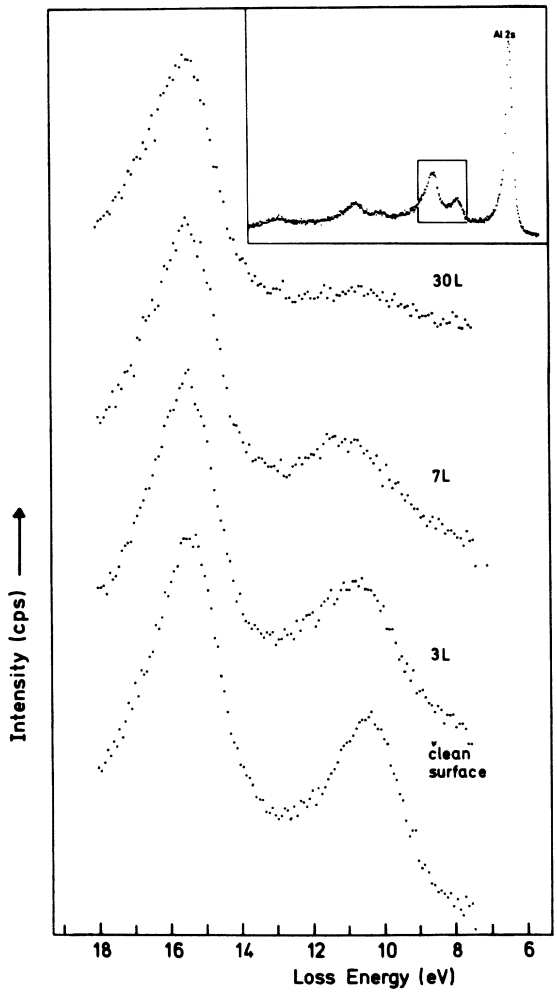

FIG. 2. Reduction of intensity of the surface plasmon satellite on the Al 2s line as a function of increasing oxygen coverage. Mean electron escape angle: 15°. Source radiation: Mg $K\alpha$. Inset: full Al 2s spectrum showing multiple plasmon excitations.

readily on the aluminum 2s and 2p levels as shown in Fig. 2. Here we observe a very sharp surface plasmon, which is already considerably reduced in intensity after exposure to 3 L oxygen (~0.1 ML). Previously published XPS spectra from ultrahigh-vacuum deposited aluminum films[6,9,10,32,33] show a less pronounced surface plasmon, which may thus be due to contamination effects. Alternatively, the mean photoelectron escape angle may have been considerably higher in these experiments. A chemisorption-induced attenuation of fast electron surface plasmon coupling has already been observed in the hydrogen-nickel system by Christmann *et al.*[34] and in the oxygen-molybdenum system by Ballu *et al.*[31]

In order to distinguish between extrinsic and intrinsic effects in the O 1s spectrum, the angular dependence of the coupling parameter was measured. In terms of a simple model (described below) we should expect the intrinsic effect to be independent of the photoelectron escape angle. The extrinsic effect on the other hand is expected to be strongly angular dependent: at lower escape angles the photoelectron remains correspondingly longer in the surface region, thus increasing the probability of coupling via its Coulomb field. In Fig. 3 we show graphically the coupling parameter measured at five escape angles. Each measurement was repeated twice and found to be quite reproducible: the vertical error bars reflect the inaccuracy involved in determining the coupling parameter by graphical integration from spectra such as that of Fig. 1. The horizontal error bars refer to the error in the absolute mean angle determination. The relative mean angle, that is, the angle between different sample positions, was accurate to better than half a degree. The coverage was 0.17 ML (= 5 L) as in Fig. 1; identical scan conditions were also used. After each measurement the crystal was cleaned in two or more argon-bombardment–anneal cycles and redosed to 5 L oxygen for the next measurement. The strong angular dependence shown in Fig. 3 does not, however, correspond exactly to pure extrinsic behavior. The dashed line (fitted to the experimental points at 7.5° and 15°) represents the $1/\sin\theta$ dependence of the extrinsic model (see

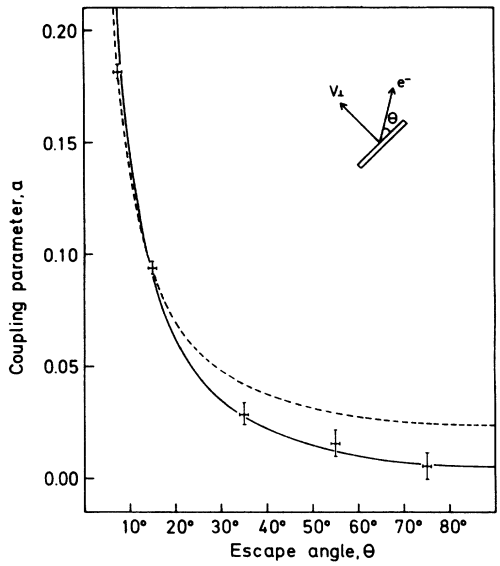

FIG. 3. Measured angular dependence of the coupling parameter a (see text) at a coverage of approximately 0.17 monolayers. The dashed line gives the angular dependence expected for pure extrinsic coupling fitted to the experimental values at 7.5° and 15°. The full line represents the best fit obtained with Eq. (23).

below). At higher escape angles the experimental points lie below this line, indicating that the measured coupling parameter is attenuated more rapidly at increasing escape angles than is expected on the basis of a purely extrinsic model.

III. DISCUSSION

A comprehensive theoretical description of plasmon effects in the energy-loss spectra of fast electrons has been given by Šunjić and Lucas.[35] The core hole plasmon coupling in x-ray photoelectron spectroscopy (XPS) and related experiments has been discussed by various authors.[14,36–39] In the context of XPS Chang and Langreth[37] introduced the concept of "intrinsic" and "extrinsic" plasmon effects. The intrinsic effect is due to the core-hole plasmon coupling, while the extrinsic effects result from the coupling of the outgoing fast electron to the plasmon field. The importance of interference effects also has been extensively discussed.[37,38]

In interpreting the experimental results described above we can thus build on a well-established theoretical picture. Here we are mainly interested in the analysis of the plasmon effects in the photoemission from the adsorbate. In this case the core hole and the outgoing electron do not couple to the volume plasmon but, as we have seen, only to the surface plasmon. It suffices, therefore, to consider the Hamiltonian of the perturbed surface plasmon field[35,36,38]:

$$H=\sum_{\vec{q}}\omega_s b_{\vec{q}}^{\dagger}b_{\vec{q}}+\Theta(t)\sum_{\vec{q}}(g_{\vec{q}}^{i}+g_{\vec{q}}^{e})(b_{\vec{q}}+b_{-\vec{q}}^{\dagger}), \tag{1}$$

where $b_{\vec{q}}^{\dagger}$, $b_{\vec{q}}$ are creation and annihilation operators for surface plasmons of wave vector $\vec{q}$ (parallel to the surface) and ω_s is the surface-plasmon frequency (its dispersion is neglected for simplicity). $g_{\vec{q}}^{i}$ and $g_{\vec{q}}^{e}$ represent the coupling of the core hole and of the photoelectron to the surface plasmons. Since the core hole is localized and since the outgoing electron is sufficiently fast in the experiment described here, recoil effects can be neglected to a good approximation.[35,36]

To determine the coupling constants we have to calculate the interaction energy of the corresponding external sources with the surface plasmon field. The electrostatic potential set up by the plasmon field is [4,27]

$$\phi(\vec{r})=\sum_{\vec{q}}\left(\frac{4\pi\omega_s}{qF}\right)^{1/2}e^{-q|z|}e^{i\vec{q}\cdot\vec{\rho}}, \tag{2}$$

where $\vec{\rho}$ is the two-dimensional position vector in the surface (which is taken to be the x-y plane), F is the total surface area and $q=(q_x^2+q_y^2)^{1/2}$.

From the Poisson equation, the potential corresponds to a charge distribution

$$\sigma(\vec{r})=\sum_{\vec{q}}\frac{q}{2\pi}\left(\frac{4\pi\omega_s}{qF}\right)^{1/2}e^{i\vec{q}\cdot\vec{\rho}}\,\delta(z). \tag{3}$$

With Eq. (2) the coupling constant for a moving point charge described by

$$\sigma_e(\vec{r},t)=e\delta(\vec{\rho}-\vec{\rho}_e(t))\delta(z-z_e(t)) \tag{4}$$

is easily determined:

$$\begin{aligned}g_{\vec{q}}&=\int d^3r\,\sigma_e(\vec{r})\phi(\vec{r})\\&=e\left(\frac{\pi\omega_s}{qF}\right)^{1/2}e^{-q|z_e(t)|}e^{i\vec{q}\cdot\vec{\rho}_e(t)}.\end{aligned} \tag{5}$$

For a free outgoing photoelectron we have

$$\rho_e(t)=\vec{v}_{\parallel}t,\quad z_e(t)=z_0+v_{\perp}t, \tag{6}$$

where z_0 is the adsorbate-surface distance, and thus the extrinsic coupling constant

$$g_{\vec{q}}^{e}=-\left(\frac{\pi e^2\omega_s}{qF}\right)^{1/2}e^{-qz_0}e^{-qv_{\perp}t}e^{i\vec{q}\cdot\vec{v}_{\parallel}t}. \tag{7}$$

After approximating the core-hole charge distribution by a positive point charge at distance z_0 from the surface, the intrinsic coupling constant also follows from Eq. (5)

$$g_{\vec{q}}^{i}=(\pi e^2\omega_s/qF)^{1/2}e^{-qz_0}. \tag{8}$$

Equations (7) and (8) complete the definition of the model.

Using the Hamiltonian (1) the modification of the energy spectrum of the photoemitted electrons due to the coupling to the plasmon field can be calculated exactly. The transition probability per unit energy is given by[35]

$$P(\omega)=\lim_{t_0\to\infty}\sum_{f}|\langle\psi_s(t_0)|f\rangle|^2\delta(\omega-E_f+E_i), \tag{9}$$

where $|\psi_s(t)\rangle$ is the state vector of the plasmon field in the Schrödinger representation. The final state $|f\rangle$ are the eigenstates of the Hamiltonian

$$\hat{H}=\sum_{\vec{q}}\omega_s b_{\vec{q}}^{\dagger}b_{\vec{q}}+\sum_{\vec{q}}g_{\vec{q}}^{i}(b_{\vec{q}}+b_{-\vec{q}}^{\dagger}), \tag{10}$$

since $g_{\vec{q}}^{e}$ vanishes for $t\to\infty$. E_i and E_f are the initial- and final-state energies. In the present case the initial state is the ground state $|0\rangle$ of the plasmon system and thus $E_i=0$. Eq. (9) may be rewritten in the form

$$P(\omega)=\lim_{t_0\to\infty}\frac{1}{2\pi}\int dt\,e^{i\omega t}\langle\psi_s(t_0)|e^{-i\hat{H}t}|\psi_s(t_0)\rangle. \tag{11}$$

To calculate $|\psi_s(t_0)\rangle$ we change to the interaction representation:

$$|\psi_I(t)\rangle = e^{iH_0 t}|\psi_s(t)\rangle$$

with $H_0 = \sum_{\vec{q}} \omega_s b_{\vec{q}}^\dagger b_{\vec{q}}$ and the time-dependent perturbation $V = \Theta(t)\sum_{\vec{q}}(g_{\vec{q}}^i + g_{\vec{q}}^e)(b_{\vec{q}} + b_{-\vec{q}}^\dagger)$. The Schrödinger equation in the interaction representation

$$i\frac{d}{dt}|\psi_I(t)\rangle = V_I|\psi_I(t)\rangle$$

with

$$V_I = e^{iH_0 t} V e^{-iH_0 t}$$

$$= \Theta(t)\sum_{\vec{q}}(g_{\vec{q}}^i + g_{\vec{q}}^e)(b_{\vec{q}} e^{-i\omega_s t} + b_{-\vec{q}}^\dagger e^{i\omega_s t})$$

can be solved exactly, giving

$$|\psi_s(t_0)\rangle = e^{-iH_0 t_0} U|0\rangle \tag{12}$$

with

$$U = \exp\left(-i\sum_{\vec{q}}(\kappa_{\vec{q}} b_{\vec{q}} + \kappa_{\vec{q}}^* b_{\vec{q}}^\dagger)\right), \tag{13}$$

$$\kappa_{\vec{q}} = \int_0^{t_0} dt\,(g_{\vec{q}}^i + g_{\vec{q}}^e)e^{-i\omega_s t}. \tag{14}$$

With these results Eq. (11) reads

$$P(\omega) = \lim_{t_0 \to \infty}\frac{1}{2\pi}\int dt\, e^{i\omega t}\langle 0|U^\dagger e^{-i\hat{H}_I t} U|0\rangle \tag{15}$$

with

$$\hat{H}_I = \sum_{\vec{q}}\omega_s b_{\vec{q}}^\dagger b_{\vec{q}} + \sum_{\vec{q}} g_{\vec{q}}^i (b_{\vec{q}} e^{-i\omega_s t_0} + b_{-\vec{q}}^\dagger e^{i\omega_s t_0}).$$

The next step is to diagonalize $\hat{H}_I$ by the unitary transformation

$$V = \exp\left(\sum_{\vec{q}}(\lambda_{\vec{q}} b_{\vec{q}} - \lambda_{\vec{q}}^* b_{\vec{q}}^\dagger)\right),$$

$$\lambda_{\vec{q}} = -(g_{\vec{q}}^i/\omega_0)e^{-i\omega_s t_0}$$

giving

$$V\hat{H}_I V^\dagger = H_0 - \Delta E,$$

$$\Delta E = \sum_{\vec{q}}(g_{\vec{q}}^i)^2/\omega_s, \tag{16}$$

and thus

$$P(\omega) = \lim_{t_0 \to \infty}\frac{1}{2\pi}\int dt\, e^{i(\omega+\Delta E)t}\langle 0|U^\dagger V^\dagger e^{-iH_0 t} V U|0\rangle. \tag{17}$$

Using the Baker-Hausdorff formula $e^A e^B = e^{A+B+[A,B]/2}$ we have, except for an irrelevant phase factor,

$$UV = \exp\left(\sum_{\vec{q}}(\gamma_{\vec{q}} b_{\vec{q}} - \gamma_{\vec{q}}^* b_{\vec{q}}^\dagger)\right)$$

with

$$\gamma_{\vec{q}} = \lambda_{\vec{q}} - i\kappa_{\vec{q}}$$

$$= \left(\frac{\pi e^2}{qF\omega_s}\right)^{1/2} e^{-qz_0}\left(\frac{\omega_s}{\omega_s - \vec{q}\cdot\vec{v}_\parallel - iqv_\perp} - 1\right)$$

for $t_0 \to \infty$. (18)

Inserting the complete set of eigenstates $|n\rangle$ of H_0 into Eq. (17) the matrix elements $\langle n|UV|0\rangle$ can be evaluated in a straightforward way, giving the final result

$$P(\omega) = \sum_{n=0}^{\infty}\frac{e^{-a}a^n}{n!}\,\delta(\omega - \Delta E - n\omega_s) \tag{19}$$

with the coupling parameter

$$a = \sum_{\vec{q}}|\gamma_{\vec{q}}|^2. \tag{20}$$

Equation (19) describes the plasmon effects in the energy spectrum of the photoemitted electrons. The kinetic energy of the photoelectrons is shifted by an amount ΔE which is just the screening energy of the core hole. In addition, the spectrum exhibits plasmon satellite lines with a Poisson-like intensity distribution. The coupling parameter a gives the intensity of the first plasmon satellite relative to the no-loss line. While the energy shift ΔE depends only on the core-hole plasmon coupling constant $g_{\vec{q}}^i$, the intensity of the satellite lines depends on both $g_{\vec{q}}^i$ and $g_{\vec{q}}^e$ and thus on the velocity of the photoelectrons. Equations (18) and (20) reveal clearly the interference between the extrinsic and intrinsic couplings in the XPS experiment. For $v \to 0$ the plasmon satellites vanish altogether and only the relaxation shift remains. In the other extreme, $v \to \infty$, the extrinsic coupling vanishes. In this case

$$\int d\omega\,\omega P(\omega) = 0,$$

i.e., the center of gravity of the energy spectrum coincides with the energy the photoelectrons would have had in the absence of any plasmon effects.

To demonstrate explicitly the velocity dependence of the coupling parameter a, the $\vec{q}$ summation in Eq. (20) remains to be done. From Eqs. (18) and (20) we have

$$a = \frac{e^2}{4\pi\omega_s}\int_0^{q_c} dq \int_0^{2\pi} d\phi\, e^{-2qz_0}\left[1 + \frac{\omega_s^2}{(\omega_s - qv_\parallel\cos\phi)^2 + q^2 v_\perp^2} - \frac{2\omega_s(\omega_s - qv_\parallel\cos\phi)}{(\omega_s - qv_\parallel\cos\phi)^2 + q^2 v_\perp^2}\right], \tag{21}$$

where the first term in the square brackets represents the pure intrinsic effect, the second term the pure extrinsic effect, and the third term the interference between both. q_c is the surface plasmon cutoff wave vector.

In the limit of large photoelectron velocity ($vq_c/\omega_s \gg 1$) the evaluation of the integrals in Eq. (21) becomes simpler: since in the second and third term of Eq. (21) only small q values contribute significantly, we may replace e^{-2qz_0} by unity and extend the q integral to infinity, giving

$$a = a_1 + a_2 + a_3 = \frac{e^2 q_c}{2\omega_s}\,\frac{1-e^{-2q_c z_0}}{2q_c z_0} + \frac{\pi e^2}{4v_\perp} - \frac{\pi e^2}{2v}\,. \tag{22}$$

Note that the extrinsic effect (a_2) varies as $1/\sin\theta$, where θ is the angle between the photoelectron velocity and the surface, whereas the interference term (a_3) is independent of θ (in the limit of high velocity). The pure intrinsic coupling (a_1) is of course independent of θ, but depends sensitively on the cutoff q_c and the adatom-surface distance z_0.

In Fig. 4 the coupling parameter a and its components a_1, a_2, and a_3 are plotted as a function of θ for photoelectrons of kinetic energy $E_{kin} = 730$ eV as in the present experiment. The cutoff wave vector has been chosen to be $q_c = 0.6$ a.u.$^{-1}$, as determined theoretically by Inglesfield and Wikborg,[40] and $z_0 = 1$ Å, which is considered as a representative value for oxygen chemisorbed on aluminum. Note that z_0 is the distance from the effective image plane and thus not necessarily identical with the distance between the oxygen ion core and the first plane of aluminum ion cores.

Comparing Fig. 4 with the experimental data given in Fig. 3, two observations are of interest. Firstly, the absolute magnitude of the plasmon effects is much weaker than predicted by our model. Secondly, the angular dependence of the coupling parameter as predicted by the model differs considerably from that observed experimentally. Since for small angles θ the coupling is dominated by the extrinsic effect, which varies as $1/\sin\theta$, one can fit a curve to the experimental data at small θ (dashed line in Fig. 3). At large angles the experimental coupling strength is seen to drop considerably below this curve. In the theoretical model, however, the coupling parameter is for reasonable values of z_0 always larger than that predicted by purely extrinsic coupling (see, e.g., Fig. 4). Thus the above model explains neither quantitatively nor qualitatively the experimental data.

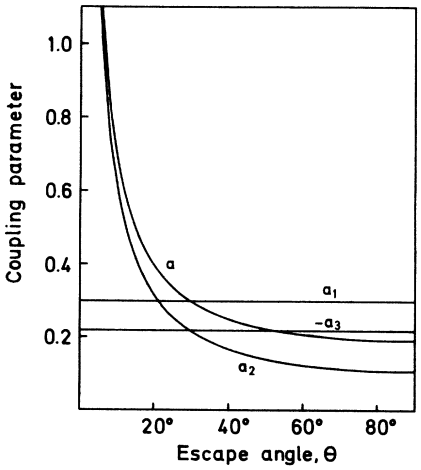

FIG. 4. Angular dependence of the coupling parameter a and its components a_1, a_2, a_3, calculated from Eq. (22) using $q_c = 0.6$ a.u.$^{-1}$, $z_0 = 1$ Å.

What can be learned from the observed angular dependence of the coupling parameter and the apparent inability of the model to explain the data? First of all it is of interest to note that scaling the intrinsic and extrinsic constants $g_{\vec{q}}^{i}$ and $g_{\vec{q}}^{e}$ *separately* by a factor (i.e., introducing adjustable effective charges Z_i^{eff} and Z_e^{eff} for the hole and the photoelectron, respectively) does not allow a fit to the observed data for any reasonable choice of z_0. This proves that the $\vec{q}$ dependence of $g_{\vec{q}}^{i}$ and/or $g_{\vec{q}}^{e}$ must deviate from that given by the model.

On the other hand the θ dependence of the three terms in Eq. (22) should hold quite generally in the high-velocity limit (in the present experiment $vq_c/\omega_s \approx 10$, i.e., the high-velocity limit pertains to a good approximation). To make further progress, we must consider the different dependence of the extrinsic and intrinsic coupling constants on $\vec{q}$. As can be seen from Eq. (21) only the small values of q contribute to the extrinsic and the interference term since v is large, whereas (for $q_c z_0 \lesssim 1$) all values of q up to the cutoff q_c contribute to the intrinsic term. Therefore the relative strength of a_2 and a_3 should be well represented by Eq. (22), while a_1 should be treated independently in a more general *ansatz*. Therefore, at least for high velocities, the following expression is the appropriate extension of Eq. (22)

$$a = c_1\left(c_2 + \frac{\pi e^2}{4v\sin\theta} - c_3\frac{\pi e^2}{2v}\right). \tag{23}$$

As mentioned above, $c_3 \approx 1$ for sufficiently high velocities. The meaning of the two new parameters c_1 and c_2 is as follows. Since the mechanism of the coupling of the fast electron to the plasmon field is probably well described by our idealized model leading to Eq. (22), the deviation of c_1 from unity represents the extent to which the properties of the true plasmons differ from those they have

in the idealized model. Thus possible imperfect screening due to the discrete atomic structure of the aluminum surface will be absorbed into the parameter c_1. As described above, the coupling strength is found to be strongly coverage dependent. The coverage dependence, reflecting the disturbance of the surface plasmons by the adsorbate, is also contained in c_1. The second parameter c_2 in Eq. (23) describes the relative magnitude of the pure intrinsic effect.

Since we are not in a position to calculate sufficiently accurate values for c_1 and c_2 from first principles, we shall evaluate them by fitting the experimental data. The full curve in Fig. 3 shows the best fit to the data obtained with Eq. (23). The corresponding values of the parameters are $c_1 = 0.27$, $c_2 = 0.13$. The low value of c_1 indicates the overall weakness of the coupling. This weakness is at least partly due to the nonzero coverage in the present experiment (0.17 ML). Note that the model yields $a_1 = 0.30$ for $q_c = 0.6$ a.u.$^{-1}$ and $z_0 = 1$ Å, whereas experimentally $a_1 = c_1 c_2 \approx 0.04$. The intrinsic coupling is thus much weaker than expected from the idealized model, not only absolutely, but also relative to the extrinsic and interference terms.

It is rather improbable that the weakness of the intrinsic coupling is due to an unusually large adsorbate-surface separation. As will be seen below the low magnitude of c_2 is most naturally accounted for by introducing an effective cutoff wave vector for the intrinsic coupling. (Remember that we have shown that the $\vec{q}$ dependence of at least one of the two coupling constants must differ from that given by the model). Defining q_c^{eff} by

$$\frac{e^2 q_c^{eff}}{2\omega_s}\,\frac{1-e^{-2z_0 q_c^{eff}}}{2z_0 q_c^{eff}} = c_2 ,$$

we obtain for $z_0 = 1$ Å

$$q_c^{eff} = 0.22 q_c = 0.13 \text{ a.u.}^{-1} . \tag{24}$$

We are thus led to the conclusion that only plasmons with wave vectors smaller than about 0.13 a.u.$^{-1}$ contribute to the screening of the core hole. This estimate depends, of course, on the choice $z_0 = 1$ Å. If larger values are chosen for z_0, somewhat larger values are also obtained for q_c^{eff}.

The main result of the present analysis is that it yields an approximate value for the strength of the coupling of the O 1*s* core hole of adsorbed oxygen to the surface plasmons of aluminum: $a_1 \approx 0.04$. To the knowledge of the authors this is the first time that the presence of the intrinsic effect could be demonstrated and its magnitude quantitatively assessed. This result is of some relevance, since the strength of the intrinsic coupling parameter is directly related to the relaxation energy ΔE of the core hole due to the screening by the metal surface

$$\Delta E = a_1 \omega_s \tag{25}$$

as follows from Eqs. (16) and (22). Our results thus imply a screening energy shift of only about 0.4 eV. Of course this result holds only for the O 1*s* core hole of oxygen on Al(111) at a coverage of about 0.17 ML. It might be an indication, however, that for core holes of adsorbed atoms and molecules the relaxation energies due to screening by the plasmon field are smaller than usually assumed.[14,41]

In the following some observations are made which might explain the unexpected low magnitude of the core-hole plasmon coupling strength. The simplest idea is to take account of the fact that the cloud of the oxygen valence electrons prevents the metallic screening charge from penetrating into the atomic volume, rendering the screening of a core hole less effective than that of a point charge. This effect can be incorporated into the above theoretical model as follows. The screening energy of a point charge at distance z_0 from the surface is given by

$$W_0 = -\sum_{\vec{q}} \frac{\pi e^2}{qF} e^{-2qz_0} . \tag{26}$$

The summation over q is confined to wave vectors smaller than q_c. For $z_0 \gg q_c^{-1}$ Eq. (26) reduces to the classical image potential

$$W_0 = -e^2/4z_0 . \tag{27}$$

The induced screening charge distribution is given by

$$\sigma_i(\vec{r}) = \sum_{\vec{q}} \frac{e}{F} e^{-qz_0} e^{i\vec{q}\cdot\vec{\rho}} \delta(z) . \tag{28}$$

The interaction of this charge distribution with the effective repulsive potential $V(r)$ set up by the atomic valence electrons will reduce the screening energy by the amount

$$W_1 = \frac{1}{2e}\int d^3r\, V(\vec{r})\sigma_i(\vec{r}) = \sum_{\vec{q}} \frac{1}{2F} e^{-qz_0} V_{\vec{q}} \tag{29}$$

with

$$V_{\vec{q}} = \int d^3\rho\, V(\vec{\rho}, 0) e^{i\vec{q}\cdot\vec{\rho}} . \tag{30}$$

Defining an effective hole plasmon coupling constant g_q^{eff} by

$$W_0 + W_1 = -\sum_{\vec{q}} \frac{(g_{\vec{q}}^{eff})^2}{\omega_s} , \tag{31}$$

we have

$$(g_{\vec{q}}^{eff})^2 = (g_{\vec{q}}^{i})^2 - \left(\frac{q\omega_s}{4\pi e^2 F}\right)^{1/2} V_{\vec{q}}\, g_{\vec{q}}^{i} \tag{32}$$

with $g_{\vec{q}}^{i}$ given by Eq. (8). Self-consistency requires the correction W_1 to be proportional to $g_{\vec{q}}^{eff}$ instead of $g_{\vec{q}}^{i}$, leading to

$$(g_{q}^{eff})^2 = (g_{q}^{i})^2 - \left(\frac{q\omega_s}{4\pi e^2 F}\right)^{1/2} V_{\vec{q}}\, g_{q}^{eff} . \tag{33}$$

Eq. (33) is easily solved for $g_{\vec{q}}^{eff}$:

$$\begin{aligned} &g_{\vec{q}}^{eff} = g_{\vec{q}}^{i} f(\vec{q}) , \\ &f(\vec{q}) = [1 + (\lambda_q V_{\vec{q}}/2g_{\vec{q}})^2]^{1/2} - (\lambda_q V_{\vec{q}}/2g_{\vec{q}}) , \\ &\lambda_q = (q\omega_s/4\pi e^2 F)^{1/2} . \end{aligned} \tag{34}$$

To illustrate the effect of the reduction factor $f(\vec{q})$ we choose for the repulsive potential $V(\vec{r})$ a Gaussian distribution of strength V_0 and range r_0

$$V(\vec{r}) = V_0 \exp\{-[\rho^2 + (z - z_0)^2]/r_0^2\} \tag{35}$$

giving

$$V_{\vec{q}} = \pi V_0 r_0^2 e^{-z_0^2/r_0^2} e^{-q^2 r_0^2/4} . \tag{36}$$

Figure 5 shows a plot of the correction factor $f(\vec{q})$ for $z_0 = 1$ a.u., $r_0 = 3$ a.u. and various choices of V_0 (r_0 has been chosen to be larger than the atomic radius of oxygen to account for the fact that the actual screening charge distribution is not a δ function in z as in the present idealized model, but extends into the vacuum and thus overlaps more effectively with the charge cloud at the adsorbed atom). Figure 5 illustrates that the effect discussed here actually leads to an effective cutoff of the higher wave vector component in the coupling constant if V_0 is sufficiently large.

In the above discussion the atomic valence electrons have been represented by a static charge cloud. In fact the atomic charge distribution will relax on approximately the same time scale in which the screening by the plasmons occurs. The atomic relaxation can be considered to lead to a redistribution of the hole charge over the atomic volume. It can be easily shown that, for a delocalized charge distribution, the contribution of large wave vectors q to the screening is strongly suppressed. Atomic relaxation is thus an additional mechanism which leads to an effective cutoff wave vector q_c^{eff} for the core-hole plasmon coupling. In other words, the surface plasmon field screens only the long-range part of the potential of the core hole; the short-range part of the potential is screened by atomic and molecular relaxation, leading to the appearance of shake-up and shake-off satellites in the spectrum.

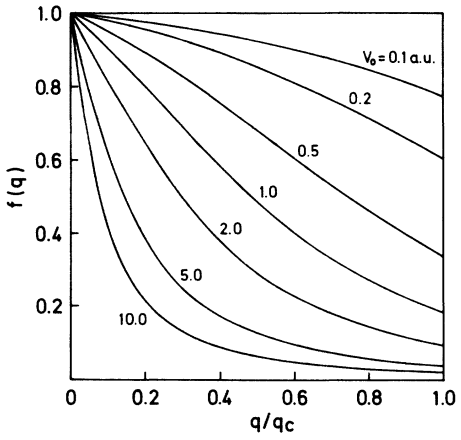

FIG. 5. Scaling factor $f(q)$, Eq. (34), as a function of wave vector q for various values of the repulsive potential V_0.

IV. CONCLUSIONS

The aluminium surface plasmon has been found to couple to the O 1s core level line in the XPS spectrum of oxygen chemisorbed on Al(111). The intensity of the surface plasmon satellite was found to be strongly coverage dependent. It seems that the metallic screening is strongly suppressed at higher coverages. The angular dependence of the plasmon loss intensity has been measured for the O 1s line and analyzed within a theoretical model. Both extrinsic and intrinsic coupling as well as the interference between the two effects could be identified. The plasmon losses are considerably weaker than predicted by the usual models. The results show clearly the importance of the interference between intrinsic and extrinsic couplings in the XPS experiment. Our analysis of the data yields a value of about 0.04 for the purely intrinsic coupling parameter, corresponding to a core-hole relaxation energy of about 0.4 eV. A simple explanation for the weakness of the core-hole–plasmon coupling has been given.

More extensive studies of the type presented here could provide us with quite detailed information on screening processes on surfaces of simple metals. From the coverage dependence of these effects we can learn more about the influence of the adsorbate on the surface plasmon. Measurements of the angular dependence of the plasmon losses are, as shown in this paper, of particular interest in this context. The concept is to use the extrinsic effect (i.e., the photoelectron-plasmon coupling), which is well understood theoretically at least for high photoelectron velocities, as a probe to study the intrinsic effect (i.e., the core-hole–plasmon coupling). The latter phenomenon is less well understood, since—as shown in the

present work—the coupling of the hole differs considerably from that of a point charge. Because the coupling constant of the outgoing electron, $g^e_{\vec{q}}$, depends both on the magnitude and the direction of the velocity, it reveals a different $\vec{q}$ dependence for different velocities and angles. Due to this fact the measurement of the angular dependence of the intensity of the plasmon losses for varying photoelectron kinetic energies would allow not only the determination of the magnitude of the intrinsic effect, but yield also information on the $\vec{q}$ dependence of the hole-plasmon coupling constant. This $\vec{q}$ dependence determines in turn the spatial distribution of the induced screening charge. Since screening effects play an important role in our understanding of chemisorption and the analysis of the photoelectron spectra of chemisorption species, the results of such measurements are of some importance.

ACKNOWLEDGMENTS

The authors would like to thank F. Dörr and E. W. Schlag for permission to complete the experimental part of this work at the Institute for Physical Chemistry of the Technische Universität München. They also acknowledge useful discussions with W. Brenig, J. Fuggle, and J. Harris. This project has been supported financially by the Deutsche Forschungsgemeinschaft through its Normalverfahren.

---

*Present address: Fakultät f. Physik der Universität Freiburg, 7800 Freiburg, West Germany.

[1]D. C. Langreth, Nobel Symp. 24, 210 (1973).
[2]D. R. Penn, J. Electron. Spectrosc. 9, 29 (1976).
[3]J. E. Houston and R. L. Park, Solid State Commun. 10, 91 (1972).
[4]A. M. Bradshaw, S. L. Cederbaum, W. Domcke, and U. Krause, J. Phys. C 7, 4503 (1974).
[5]R. L. Park, J. E. Houston, and G. E. Laramore, Jpn. J. Appl. Phys. Suppl. 2, 757 (1974).
[6]R. A. Pollak, L. Ley, F. R. McFeely, S. P. Kowalczyk, and D. A. Shirley, J. Electron. Spectosc. 3, 381 (1974).
[7]A. M. Bradshaw and W. Wyrobisch, J. Electron. Spectrosc. 7, (1975) 45.
[8]A. Barrie and F. J. Street, J. Electron Spectrosc. 7, 1 (1975).
[9]W. J. Pardee, G. D. Mahan, D. E. Eastman, R. A. Pollak, L. Ley, F. R. McFeely, S. P. Kowalczyk, and D. A. Shirley, Phys. Rev. B 11, 3614 (1975).
[10]J. C. Fuggle, D. J. Fabian, and L. M. Watson, J. Electron. Spectrosc. 9, 99 (1976).
[11]B. Lundqvist, Phys. Kondens. Mater. 9, 236 (1969).
[12]R. Manne and T. Åberg, Chem. Phys. Lett. 7, 282 (1970).
[13]L. Ley, S. P. Kowalczyk, F. R. McFeely, R. A. Pollak, and D. A. Shirley, Phys. Rev. B 8, 2392 (1973).
[14]J. Harris, Solid State Commun. 16, 671 (1975).
[15]B. Gumhalter and D. M. Newns, Phys. Lett. A 53, 137 (1975).
[16]In a recent publication [J. C. Fuggle, T. E. Madey, M. Steinkilberg, and D. Menzel, Chem. Phys. Lett. 33, 233 (1975)] a satellite at 9.6 eV was observed on the oxygen 1s peak in the adsorption system oxygen–ruthenium (001). As a satellite at 9.6 eV was also found on the clean surface ruthenium peaks a coupling to an excitation in the metal was suggested. Whether this loss corresponds to a surface plasmon is difficult to decide, because doubt exists as to the energies of the plasmons in ruthenium.
[17]See, for example, J. W. Gadzuk, Phys. Rev. B (to be published).
[18]See, for example, A. Barrie and A. M. Bradshaw, Phys. Lett. A 55, 306 (1975).
[19]A. M. Bradshaw, P. Hofmann, and W. Wyrobisch (unpublished).
[20]J. C. Fuggle, L. M. Watson, D. J. Fabian, and S. Affrossman, Surf. Sci. 49, 61 (1975).
[21]A. M. Bradshaw and J. C. Fuggle, *Proceedings of the Noordwijh Photoemission Symposium*, (European Space Agency, Noordwijh, 1976), p. 169.
[22]M. W. Roberts and B. R. Wells, Surf. Sci. 15, 263 (1969).
[23]W. H. Krueger and S. R. Pollack, Surf. Sci. 30, 263 (1972).
[24]V. J. Agarwala and T. Fort, Surf. Sci. 45, 470 (1974).
[25]K. Y. Yu, J. N. Miller, P. Chye, and W. E. Spicer, Phys. Rev. B 14, 1446 (1976).
[26]F. Jona, J. Phys. Chem. Solids 28, 2155 (1967).
[27]E. A. Stern and R. A. Ferrell, Phys. Rev. 120, 130 (1960).
[28]C. J. Powell and J. B. Swan, Phys. Rev. 118, 640 (1960).
[29]C. Kunz, Z. Phys. 196, 311 (1966).
[30]Y. Murata and S. Ohtani, J. Vac. Sci. Technol. 9, 789 (1972).
[31]Y. Ballu, J. Lecante, and H. Rousseau, Phys. Rev. B 14, 3201 (1976).
[32]Y. Baer and G. Busch, Phys. Rev. Lett. 30, 280 (1973).
[33]A. Barrie, Chem. Phys. Lett. 19, 109 (1973).
[34]K. Christmann, O. Schober, G. Ertl, and M. Neumann, J. Chem. Phys. 60, 4528 (1974).
[35]M. Šunjić and A. A. Lucas, Phys. Rev. 33, 719 (1971).
[36]D. C. Langreth, Phys. Rev. Lett. 26, 1229 (1971); Phys. Rev. B 1, 471 (1970).
[37]J. J. Chang and D. C. Langreth, Phys. Rev. B 5, 3512 (1972); 8, 4638 (1973).
[38]M. Šunjić and D. Šokčević, Solid State Commun. 15, 165 (1974); 18, 373 (1976).
[39]G. E. Laramore and W. J. Camp, Phys. Rev. B 9, 3270 (1974).
[40]J. E. Inglesfield and E. Wikborg, Solid State Commun. 14, 661 (1974).
[41]J. W. Gadzuk, J. Vac. Sci. Technol. 12, 289 (1975).